Journal of the American Heart Association

ORIGINAL RESEARCH

Dapagliflozin Improves Cardiac Hemodynamics and Mitigates Arrhythmogenesis in Mitral Regurgitation-Induced Myocardial Dysfunction

Yu-Wen Lin, PhD; Chin-Yu Chen, MD, PhD; Jhih-Yuan Shih, MD; Bor-Chih Cheng, MD; Ching-Ping Chang, PhD; Mao-Tsun Lin, PhD; Chung-Han Ho, PhD; Zhih-Cherng Chen, MD; Sudeshna Fisch, PhD; Wei-Ting Chang, MD

BACKGROUND: Mitral regurgitation (MR) is a major contributor for heart failure (HF) and atrial fibrillation. Despite the advancement of MR surgeries, an effective medical therapy to mitigate MR progression is lacking. Sodium glucose cotransporter 2 inhibitors, a new class of antidiabetic drugs, has shown measurable benefits in reduction of HF hospitalization and cardiovascular mortality but the mechanism is unclear. We hypothesized that dapagliflozin (DAPA), a sodium glucose cotransporter 2 inhibitor, can improve cardiac hemodynamics in MR-induced HF.

METHODS AND RESULTS: Using a novel, mini-invasive technique, we established a MR model in rats, in which MR induced left heart dilatation and functional decline. Half of the rats were randomized to be administered with DAPA at 10 mg/kg per day for 6 weeks. After evaluation of electrocardiography and echocardiography, hemodynamic studies were performed, followed by postmortem tissue analyses. Results showed that DAPA partially rescued MR-induced impairment including partial restoration of left ventricular ejection fraction and end-systolic pressure volume relationship. Despite no significant changes in electrocardiography at rest, rats treated with DAPA exhibited lower inducibility and decreased duration of pacing-induced atrial fibrillation. DAPA also significantly attenuated cardiac fibrosis, cardiac expression of apoptosis, and endoplasmic reticulum stress-associated proteins.

CONCLUSIONS: DAPA was able to suppress cardiac fibrosis and endoplasmic reticulum stress and improve hemodynamics in an MR-induced HF rat model. The demonstrated DAPA effect on the heart and its association with key molecular contributors in eliciting its cardio-protective function, provides a plausible point of DAPA as a potential strategy for MR-induced HF.

Key Words: apoptosis ■ cardiac fibrosis ■ dapagliflozin ■ ER stress ■ heart failure ■ mitral regurgitation ■ SGLT2 inhibitor

Mitral regurgitation (MR) is a valvular heart disease of high prevalence globally and is a known risk factor for atrial fibrillation (AF).[1–3] Although surgical interventions can arrest this pathophysiologic process to the extent of slowing down adverse cardiac remodeling, recurrence of regurgitation and AF correlates with a declining function of both left atrium (LA) and left ventricle (LV) and can lead to heart failure (HF). Given the importance of LA remodeling in disease progression, the cellular and molecular underpinnings of LA can be central to targeting a clinical therapy. Endoplasmic reticulum (ER) is a membrane system that is involved in protein folding, calcium homeostasis, and apoptosis.[4] There are 3 key signaling pathways including ATF6 (activating transcription factor 6), IRE1α (inositol-requiring protein 1 alpha), and PERK (protein kinase RNA-like endoplasmic reticulum kinase) that are induced by ER stress.[5] Under stress

Correspondence to: Wei-Ting Chang, MD, 901, Zhonghua Road, Yongkang District, Tainan, Taiwan (R.O.C.). E-mail: cmcvecho@gmail.com

Supplementary Material for this article is available at https://www.ahajournals.org/doi/suppl/10.1161/JAHA.120.019274

For Sources of Funding and Disclosures, see page 13.

JAHA is available at: www.ahajournals.org/journal/jaha

CLINICAL PERSPECTIVE

What Is New?

- Using a novel and mini-invasive rat model of mitral regurgitation, we demonstrated a cardioprotective effect of dapagliflozin on cardiac remodeling.

What Are the Clinical Implications?

- Our findings provide a plausible point of dapagliflozin as a potential strategy for mitral regurgitation-induced heart failure.

Nonstandard Abbreviations and Acronyms

A	atrial velocity
DAPA	dapagliflozin
E	transmitral early filling velocity
ER	endoplasmic reticulum
MR	mitral regurgitation

conditions such as oxidative stress, hypoxia, and calcium depletion, unfolded proteins aggregate and ER dysfunction esnsues.[6] Several reports indicated that ER stress-associated apoptosis is a contributing factor for myocardial dysfunction and AF development.[6–8] Increased expression of ER stress mediator proteins, ATF6, apoptosis-inductor CHOP (C/EBP-homologous protein), and eIF2α (eukaryotic translation initiation factor 2α) were observed in atrial tissues of patients with persistent AF.[8] The stimulation of rapid pacing could also trigger ER stress and result in increased apoptosis in HL-1 atrial myocytes through upregulating PERK/eIF2α/ATF4/CHOP pathway and downregulating antiapoptotic Bcl-2 (B cell lymphoma 2) protein.[6,9] It is critical to investigate the molecular mechanism of MR-induced ER stress and apoptosis and to explore new agents for preventing AF in patients with MR.

Dapagliflozin (DAPA), a sodium glucose cotransporter 2 (SGLT2) inhibitor, belongs to a novel class of glucose-lowering agents and is used in the treatment of patients with type 2 diabetes mellitus.[10,11] Beyond reducing glucose reabsorption and excess blood glucose elimination, DAPA has been reported to offer other protection in cardiovascular diseases.[12,13] The recently disclosed DAPA-HF trial showed that DAPA reduced the primary composite outcome including cardiovascular mortality and HF in patients with and without type 2 diabetes mellitus.[14–16] Such cardioprotective effects of DAPA have also been demonstrated in the models of diabetic cardiomyopathy, HF, and myocardial ischemia.[17–19] Despite only scant expression of SGLT2 receptors in cardiomyocytes, recent evidence supports that through modulating ER stress, SGLT2 inhibitors can mitigate myocardial dysfunction in diabetes mellitus.[20,21] However, to date, the mechanism of action of DAPA has focused mainly on its involvement in reduction of cardiac inflammation, oxidative stress, apoptosis, mitochondrial dysfunction, and ionic dyshomeostasis. The details of the molecular pathways that mediate DAPA action have remained an area of active investigation, as is the effect of DAPA treatment on patients with MR. Herein, we studied the therapeutic potential of DAPA on MR-triggered AF and cardiac remodeling. We focused on the effects of DAPA on reducing RyR2 and increasing Connexin 43 expression,[22,23] these 2 being key regulators of AF, and DAPA-mediated reduction of ER stress and apoptosis-linked molecular proteins, and explore the molecular bases of DAPA functional effect. We hope that the work warrants future research study on DAPA as a useful therapeutic agent in MR-induced HF based on our results presented here in rats subjected to MR.

METHODS

Animal Models of MR and Study Design

The data, analytic methods, and study materials that support the findings of this study are available from the corresponding author upon reasonable request. Ten-week-old adult male Sprague–Dawley rats, weighing 250 to 330 g, were used in these experiments. The rats were given free access to tap water and standard rat chow and housed in a room with a 12/12-hour light cycle. The animal experiments were approved and conducted in accordance with the strict guidelines of the Subcommittee on Research Animal Care of Chi-Mei Medical Center and the standards meet the guidance of *Guide for the Care and Use of Laboratory Animals*. The rats were anesthetized with 3% isoflurane mixed with oxygen. After successful anesthesia, a 22 G needle was inserted into the LV via animal xiphoid cartilage and was advanced toward the mitral valve (MV) to create a perforating defect in the leaflet under the echocardiographic guidance. After surgery, the regurgitant jet area of LA was detected by the color Doppler imaging. MR was considered significant if a regurgitant jet area occupied more than 45% of the LA. Two weeks after the surgery, development of MR was confirmed along with LV dilation and the rats were randomly assigned to Sham, Sham+DAPA, MR, and MR+DAPA (10 mg/kg per day for 6 weeks by oral) groups. The survival rate, body weight, blood sugar, cardiac function, and the hemodynamic parameters were measured every 2 weeks in the studied rats for a total of 8 weeks. Blood was collected via tail vein sampling for blood sugar measurement.

Before measurement, rats were fasted for 12 hours and were placed under temporal anesthesia by isoflurane, during blood samplings. The detailed experimental design is shown in Figure 1.

Measurements of Echocardiography and Electrocardiography

Cardiac function experiments were performed 1 day before and 2, 4, 6, and 8 weeks after the MR surgery guided by the GE Vivid S6 Dimension echocardiography platform with a 10 MHz linear array transducer (GE-Vingmed Ultrasound AS, Horten, Norway). Rats were anesthetized with 3% isoflurane mixed with oxygen to minimize the effects on heart rate. Throughout the procedure, heart rate was maintained above 200 beats/min, and images were recorded at a frame rate of 300 to 350/seconds. Measurements included long- and short-axis views, with ECG gating. Left ventricular M-mode 2-dimensional echocardiography was performed in parasternal short axis view to measure LA diameter, aortic annulus, left ventricular wall thickness, and chamber dimensions (interventricular septum thickness in diastole and systole), left ventricular internal diameter in diastole and systole, ejection fraction, fractional shortening, and vena contracta for the systolic function of the LV. Using apical 4 chamber view we measured transmitral early filling velocity (E), atrial velocity (A). Additionally, tissue Doppler derived early (e′) annular diastolic velocities for diastolic function of the LV were obtained.

ECG was recorded with PowerLab converter (Millar Instruments, Houston, TX) and analyzed with the LabChart (AD Instruments, Dunedin, New Zealand) system. Rats were anesthetized with 3% isoflurane mixed with oxygen to minimize the effects on heart rate. Lead II ECG was collected by connecting needle electrodes to the 4 limbs of the animal. P wave was recorded until its return to the isoelectric baseline. QRS duration was measured from the beginning of the Q wave to the peak amplitude of the downward deflection of the S wave. PR interval was measured from the beginning of the upstroke of the P wave until the maximal amplitude of the R wave. RR interval was measured as the time between consecutive R wave peaks. QT interval was measured from the beginning of the Q wave until the T wave returned to the isoelectric baseline.

Hemodynamic Study of Pressure-Volume Loop

At 8 weeks post-MR surgery, invasive hemodynamic assessments were performed using a Millar pressure catheter (SPR-838; Millar Instruments). The rats were anesthetized with an intraperitoneal injection of urethane (500 mg/kg ip). The right carotid artery of the rat was cut down to insert the microtip 2.0 F pressure-volume catheter into the LV cavity. The left jugular vein was cannulated for hypertonic saline (10%) infusion to determine the conductance. The inferior vena cava was exposed for the occlusion

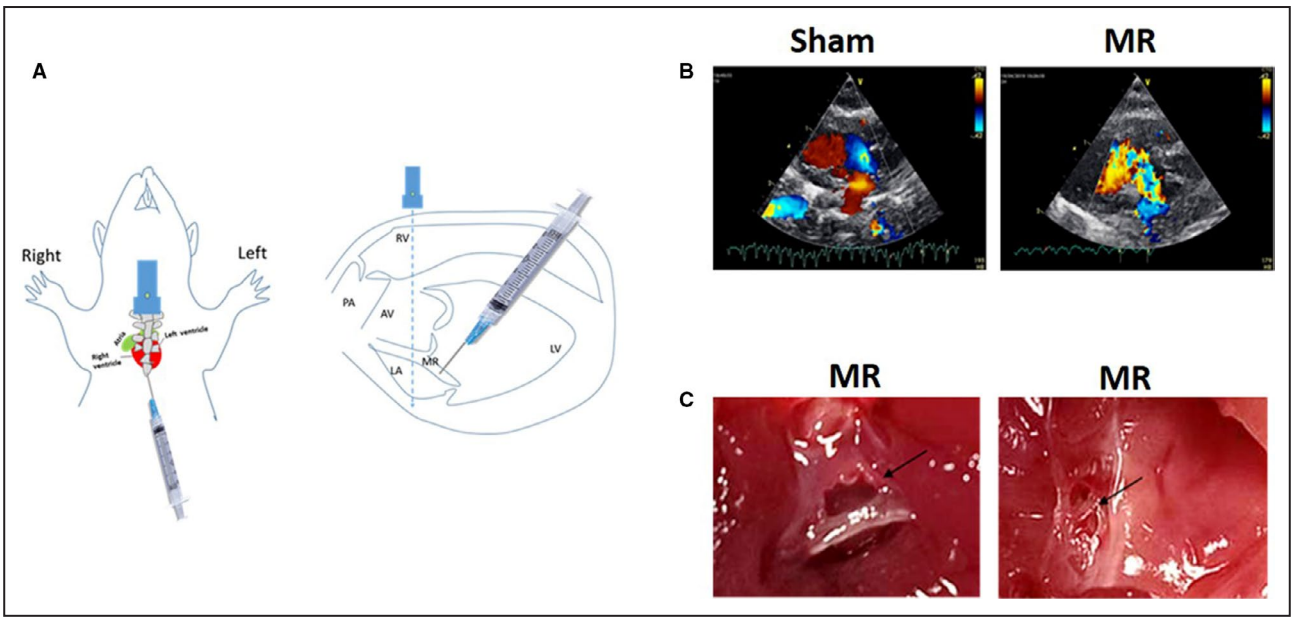

Figure 1. The establishment of mitral regurgitation (MR) in rats using echo-guided mini-invasive puncture (22G needle) technique.

A, An illustration of echocardiography guided approach of MR creation using a needle puncture via left ventricular apex. **B**, At parasternal long axis view, the mitral regurgitant jet backward into left atrium was observed immediately after the puncture using color Doppler echocardiography. **C**, In the postmortem study, 1 significant hole was noticed at the anterior leaflet of the mitral valve (arrow).

of inferior vena cava using a 3-0 surgical silk. After stabilization, the hemodynamics of LV were recorded using the PowerLab converter (Millar Instruments). The LV systolic function was evaluated by end-systolic, end-systolic, maximal velocity of pressure rise (+dP/dt) and fall (−dP/dt), arterial elastance, and end-systolic pressure-volume relationship. The LV diastolic function was evaluated by end-diastolic volume, end-diastolic pressure, the time constant of isovolumic pressure decay (tau), and end-diastolic pressure-volume relationship.

Programmed Atrial Burst Pacing for AF Provocation

After 8 weeks of MR, hearts were harvested and perfused through the aorta with Tyrode's buffer (130 mmol/L NaCl, 5.4 mmol/L KCl, 1.8 mmol/L $CaCl_2$, 1 mmol/L $MgCl_2$, 0.3 mmol/L Na_2HPO_4, 10 mmol/L HEPES, and 10 mmol/L glucose; pH adjusted to 7.4) equilibrated with a 95% O_2 and 5% CO_2 gas mixture at 37°C. The isolated hearts were perfused with warm Tyrode's solution at a rate of 10 to 12 mL/min for 5 minutes before electrical stimulation. Silver bipolar electrodes coated with Teflon except at the tip were placed on the LA. Burst LA sequentially pacing with a frequency of 3 to 10 Hz (pulse height 1V, pulse width 15 ms) for 3 to 5 seconds. The inducibility of AF and maintaining duration were recorded.

Histology of Rat Hearts

After end of experiment, rats were euthanized and fresh heart tissues were harvested. The hearts were weighed. Each heart was dissected transversely and used as follows: half of it was collected for histology and staining and the other half for molecular analyses such as Western blotting. For histopathological examination, the heart tissue was fixed in 4% paraformaldehyde and embedded in paraffin (Alfa Aesar, Lancashire, UK). The tissue sections were stained with hematoxylin-eosin and Masson's trichrome stain for evaluation of the level of fibrosis. The percentage of fibrosis in LV area was quantified by identifying and counting the number of blue-staining pixels using Image J software.

TUNEL Staining

Cardiac apoptosis was measured using heart tissues by terminal deoxynucleotidyl transferase-mediated deoxyuridine triphosphate nick end labeling assay (TUNEL [terminal deoxynucleotidal transferase–mediated biotin–deoxyuridine triphosphate nick-end labeling]; BioVision, Milpitas, CA) according to the manufacturer's protocol. In brief, formalin-fixed, paraffin-embedded tissue sections were mounted on glass slides. After de-paraffinizing the slides with xylene and ethanol, slides were microwaved for 10 minutes with Citrate Buffer (pH 6.0). The heart sections were digested with fresh diluted proteinase K (20 mg/mL) at room temperature for 10 minutes. Then, TUNEL reaction mixture containing terminal deoxynucleotidyl transferase and fluorescein-deoxyuridine triphosphate was added to each section and allowed to settle at room temperature for 30 minutes in a dark room. The sections were rinsed 3 times in PBS for 5 minutes each. The slides were counterstained with 4', 6-diamidino-2-phenylindole (DAPI, Vector Laboratories). The sections were examined under a fluorescence microscope (Olympus BX51, Olympus Optical Co. Ltd, Tokyo, Japan) to determine the percentage of apoptotic cells. Ten sections per heart were selected randomly for analysis and the analysis was performed in a blinded manner. The number of positive cells and the total number of cells were counted for 3 fields at ×200 magnification. The results are presented as the ratio of positive to total cells.

Western Blot

Equal amount of protein, extracted from heart tissues, was separated by 8% to 15% sodium dodecyl sulfate-polyacrylamide gel electrophoresis, transferred onto P polyvinylidene fluoride microporous membranes (Merck Millipore, MA, USA) and blocked in 5% milk prepared in Tris buffered solution (pH 7.6) in preparation for Western blotting. The membranes were incubated with the primary antibodies against BAX (1:1000, Cell Signaling, Danvers, MA, USA), BCL2 (1:1000, Arigo Hsinchu, Taiwan, ROC), cleaved caspase 3 (1:1000), p-PERK (phospho-PERK, 1:1000), eIF-2α (1:1000), ATF4 (1:1000), CHOP (1:500, Cell Signaling), or GAPDH (glyceraldehyde 3-phosphate dehydrogenase; 1:5000, Sigma-Aldrich Co., St Louis, MO, USA) overnight at 4°C. Finally, they were incubated with horseradish peroxidase-conjugated anti-rabbit/mouse IgG (1:5000, Merck Millipore and Sigma-Aldrich Co.) for 1 hour at room temperature. Signal were detected by ECL-Western blotting system (AVEGENE CHEMX 400). The intensity of the protein band was quantified by Image J software (National Institutes of Health, Bethesda, MD, USA) and the results were expressed after normalization to the housekeeping gene GAPDH.

Statistical Analysis

Given the small sample size, differences among the Sham and MR groups before and after DAPA treatment were compared using nonparametric tests for nonnormally distributed continuous variables and tests for categorical variables. Group differences were analyzed using Kruskal-Wallis test, including Dunn's post hoc analysis and multiple testing adjustment. A

2-tailed $P<0.05$ was considered statistically significant for all tests. All analyses were performed using SAS software version 9.4 (SAS Institute, Cary, NC, USA). Kaplan–Meier curves were plotted using STATA (version 12; Stata Corp., College Station, TX, USA).

RESULTS

DAPA Mitigated MR-Induced Left Atrial Dilatation and Left Ventricular Dysfunction

In order to investigate effects of DAPA on MR-induced cardiac remodeling, we established a novel MR model in SD rats by creating a puncture-based valve defect on the mitral leaflet through an echo-guided method (Figure 1A). After surgery, a pronounced, regurgitant jet was produced in the MR model, compared with the Sham rats (Figure 1B). In the postmortem study, the structural defect at the anterior leaflet of the MV was clearly observed specifically in the MR rats (Figure 1C). Indeed, this puncture-based surgery requires technical dexterity of the surgeon and precision of echo-guided techniques being undertaken. In an earlier pilot study, about half of the rats died immediately because of cardiac tamponade but after repeated practice and adjustment of technique, currently the immediate mortality in the surgeon's hands is <10%. In this study, for example, we originally included 14 rats for the MR group. After 2 rats died of tamponade during MR surgery, and the other 2 were excluded given that only mild MR developed following induction, eventually we had 10 rats that were followed longitudinally, after being assigned to the MR group (Figure 2). Two weeks after the surgery, as the severity of MR pathology stabilized, the rats were administered DAPA for 6 consecutive weeks. Notably, upon weekly measurements, we observed lower body weights of those MR and MR+DAPA rats compared with the Sham rats (Figure S1A). Also, the rats treated with DAPA, specifically, presented with a slight reduction of blood sugar (Figure S1B) whereas there was no corresponding significant change in heart rate or blood pressure among the study groups (Figure S1C through S1F).

Through sequential echocardiography, we measured cardiac function in Sham, Sham+DAPA, MR, and MR+DAPA rats. The representative echocardiographic images are shown in Figure 3A. Compared with the Sham and Sham+DAPA group, LA dimensions and interventricular septum thickness in diastole were significantly increased in the rats that underwent MR surgery and decreased by DAPA treatment (Figure 3B). There was no difference observed in aortic diameter among Sham, Sham+DAPA, MR, and MR+DAPA rats (Figure 3C). With regard to LV remodeling, DAPA treatment significantly decreased the MR-enlarged chamber size (left ventricular internal diameter in diastole) but did not alter the LV hypertrophy (interventricular septum thickness in diastole) (Figure 3D and 3E). Also, in the DAPA-treated rats, ejection fraction, fractional shortening, and vena contracta all significantly improved as compared with the untreated MR rats (Figure 3F through 3H). As per the effect on diastolic dysfunction, although DAPA mitigated the MR-induced increase of MV inflow (E velocity of Sham, MR, and MR+DAPA seen as 99.9±10.9 cm/s, 165.7±14.5 cm/s, and 142.6±43 cm/s, respectively, $P=0.04$), there was no significant change in other diastolic parameters (Figure S2). Given that DAPA did not alter structural and functional parameters in the control groups (Sham and Sham+DAPA), we mainly focused on 3 groups—Sham, MR, and MR+DAPA in the following hemodynamic, histologic, and molecular studies.

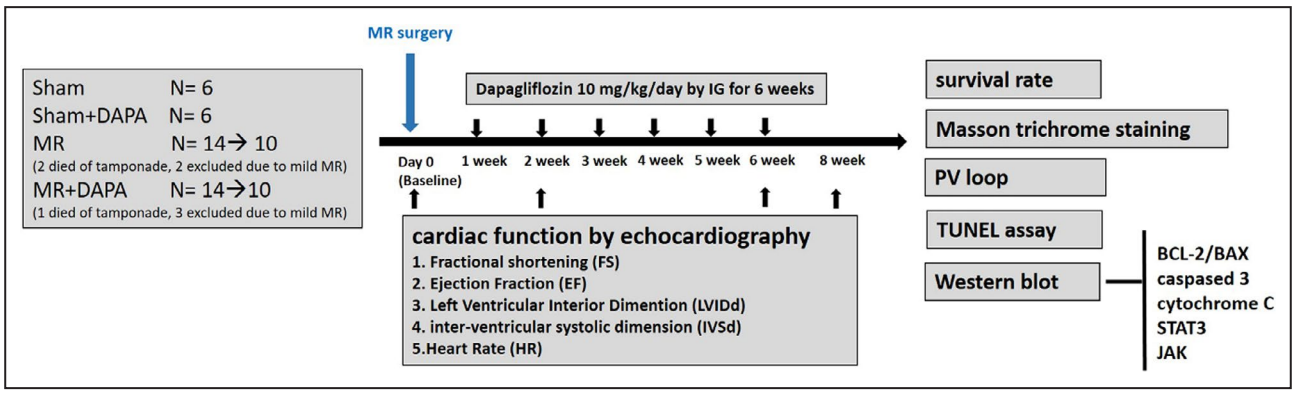

Figure 2. The study design of dapagliflozin on cardiac remodeling in rats with mitral regurgitation (MR).
After the surgery of MR, the rats received dapagliflozin at 10 mg/kg per day for 6 weeks orally. The heart rate, blood pressure, and cardiac function were observed by echocardiography every 2 weeks. At the end of the experiments, the section of heart were stained using Masson trichrome for the quantification of myocardial fibrosis. The apoptotic effect in heart tissue was measured by TUNEL (terminal transferase-mediated dUTP nick-end labeling) staining. The apoptosis- and endoplasmic reticulum stress-associated protein were measured by Western blot. DAPA indicates dapagliflozin; and PV, pressure-volume.

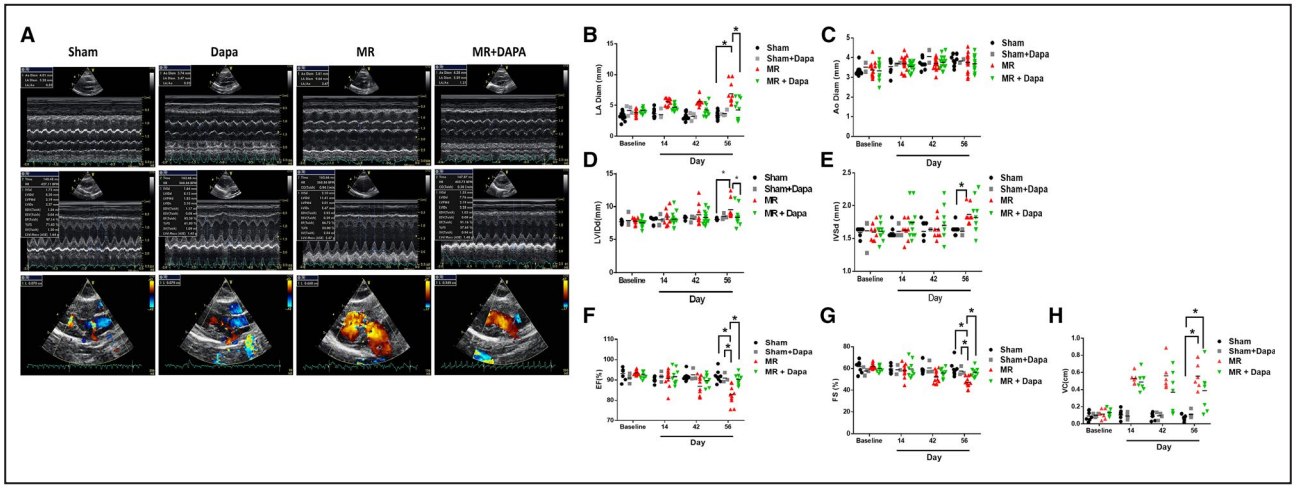

Figure 3. Dapagliflozin (DAPA) partially rescued mitral regurgitation (MR)-induced myocardial dysfunction in echocardiographic assessments.

A, Sequential measurements of echocardiography are shown in the Sham, Sham+DAPA, MR, and MR+DAPA groups; (**B**) Echocardiographic measurements of left atrium (LA) diameter, (**C**) aorta diameter, (**D**) left ventricular internal dimension at end-diastole (LVIDd), (**E**) interventricular septal thickness at end-diastole (IVSd), (**F**) ejection fraction (EF), (**G**) fractional shortening (FS), and (**H**) vena contracta (VC) are shown for each group. Data are expressed using mean±SD. Kruskal-Wallis test and Dunn's post hoc analysis for analysis of group differences. *P<0.05 for difference from each group. (N=6–12).

DAPA Improves MR-Induced Volume Overload in Hemodynamic Studies

We investigated the effect of DAPA on the changes in hemodynamics in rats with MR and assessed pressure-volume relationships among different groups of rats. Figure 4A shows representative results of the pressure-volume loop analyses with different preload conditions in Sham, MR, and MR+DAPA rats. As seen in Figure 4B, compared with the Sham, both end-systolic volume and end-diastolic volume were higher in MR rats and this effect was partially reversed by DAPA treatment. Similarly, maximal velocity of pressure rise (+dP/dt) and fall (–dP/dt) was suppressed in MR rats and mitigated by DAPA treatment (Figure 4C). There was no significant change in arterial elastance and isovolumic pressure decay (tau) (Figure 4D). Through temporal clamping the abdominal inferior vena cava, we found that although the end-diastolic pressure-volume relationship was not significantly different among the groups, end-systolic pressure-volume relationship was blunted specifically in MR rats, and again, this effect was reversed by DAPA (Figure 4E). Our findings imply that DAPA mitigates the hemodynamic suppression in rats subjected to MR and can partially restore hemodynamic balance in the surgically induced MR model.

DAPA Suppressed the Inducibility and Maintenance of Tachypacing-Induced AF

As previously reported,[24] MR may lead to the development of AF through LA volume overload, progressive atrial fibrosis, and electro-anatomic remodeling. Thereby, we measured the surface ECG to assess the effect of DAPA on electrical remodeling after MR injury. There was also no significant difference among the study groups in PR or RR intervals, QRS duration, and QTc intervals, at rest (Figure S3). Using ex vivo atrial burst pacing, we placed silver bipolar electrodes at LA of the isolated and perfused rat heart (Figure 5A). Through sequentially pacing LA with a frequency of 3 to 10 Hz for 3 to 5 seconds, we successfully induced AF (Figure 5B). After termination of the burst phase, irregular atrial rhythm with irregular ventricular response was observed as a typical ECG of AF. LA burst-stimuli transiently induced AF in 16% of the Sham rats. The development of MR aggravated the inducibility of AF up to 85% and was suppressed in 28% by DAPA treatment in rats (Figure 5C). Average AF duration was longer in the MR rats than in the Sham rats (6.18±5.35 seconds versus 99.2±46.51 seconds). DAPA treatment significant diminished AF duration in 26.5±46.26 (Figure 5D).

To investigate whether known AF associated proteins are activated, we analyzed the expression of RyR2, major calcium channel protein identified in AF development.[22] Compared with Sham rats, the levels of pRyR2 proteins increased about 5-fold in the left atrial tissue of MR rats and the upregulation was suppressed by DAPA treatment (Figure 5E). The levels of Connexin 43, a gap junction protein that is most commonly expression in atrial myocytes, were also

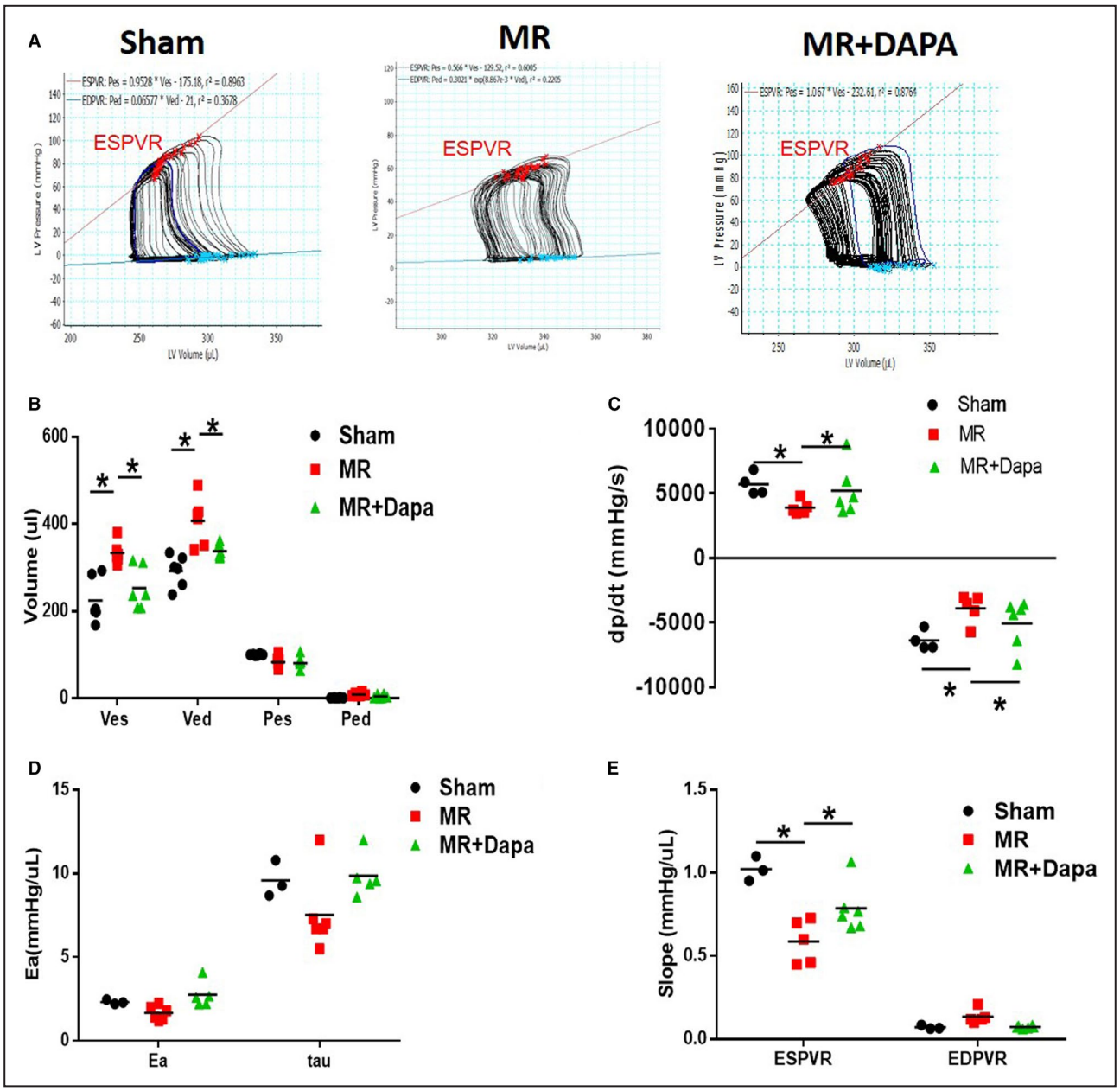

Figure 4. Dapagliflozin (DAPA) attenuated mitral regurgitation (MR)-induced hemodynamic decline in rats.
A, Representative pressure-volume images in the Sham, MR, and MR+DAPA groups were obtained from Millar catheterization. Hemodynamic measurements obtained in the 3 groups are shown in (**B**) the mean end-systolic volume (Ves), end-diastolic volume (Ved), end-systolic pressure (Pes), and end-diastolic pressure (Ped), (**C**) maximal velocity of pressure rise (+dP/dt) and fall (−dP/dt), (**D**) mean arterial elastance (Ea), the time constant of isovolumic pressure decay (tau), (**E**) mean slopes of the ESPVR and the EDPVR are shown for each group. Data are presented as the means± SD. Kruskal-Wallis test and Dunn's post hoc analysis for analysis of group differences. **P*<0.05 for difference from each group. (N=6). EDPVR, end-diastolic pressure-volume relationship; ESPVR, end-systolic pressure-volume relationship.

measured by Western blot.[22,23] The left atrial expression of Connexin 43 was found significantly lower in MR rats (≈45% reduction) than in Sham rats whereas DAPA treatment significantly increased the Connexin 43 expression in MR+DAPA rats (Figure 5E). Our findings imply that DAPA can attenuate LA inducibility and duration of AF, and the mechanism involves reduction in levels of RyR2 and increase in levels of Connexin 43, specifically seen in study rats subjected to MR.

DAPA Attenuated Cardiac Fibrosis in Ventricular Tissues

There was one rat in MR group and another in the MR+DAPA that died during the follow-up duration,

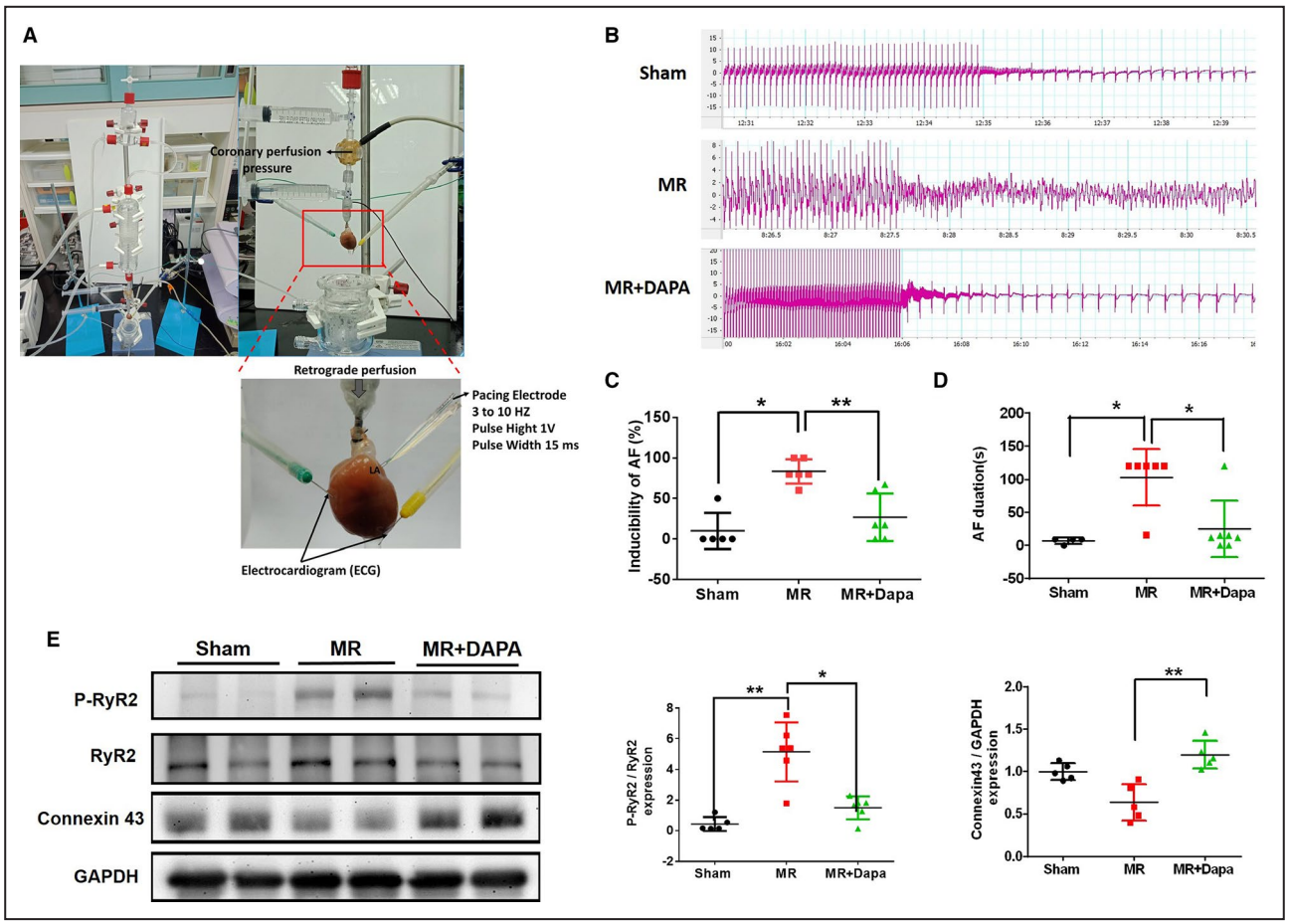

Figure 5. Dapagliflozin (DAPA) suppressed the MR-triggered atrial fibrillation (AF) and the upregulation of arrhythmogenic protein expressions in rats.
A, The illustration of retrograde perfusion, ECG recordings, and programmed atrial burst pacing for AF provocation. **B**, Representative AF episodes after atrial burst pacing are shown in the Sham, MR, and MR+DAPA groups. **C**, The inducibility and (**D**) duration of AF, in each group, was measured. **E**, The expression of pRyR2/RyR2 ratio and Connexin 43 was evaluated by western blot. The relative expression level of each protein was quantified by densitometry and normalized to the GAPDH (glyceraldehyde 3-phosphate dehydrogenase) level. Data are expressed using mean± SD. Kruskal-Wallis test and Dunn's post hoc analysis for analysis of group differences. **P*<0.05, and ***P*<0.01 for difference from each group. (N=3–6).

but no other significant difference in mortality was observed in Sham, MR, and MR+DAPA rats (Figure 6A). No significant difference in heart to body weight ratio was seen between the MR and MR+DAPA groups but the increased ratio of the wet to dry lung in rats of MR was reversed after the treatment with DAPA (Figure 6B through 6E). The morphology of hearts in each group was measured by hematoxylin-eosin staining (Figure 6F) and Masson trichrome staining detected myocardial fibrosis (Figure 6G). Compared with Sham rats, fibrosis in LV region was significantly increased in MR rats whereas DAPA attenuated LV fibrosis (Figure 6H). Relative to Sham rats, the fibrosis levels of MR rats were seen as substantially increased, by ≈4.4-fold. For MR+DAPA rats, there was a significant reduction (≈1.8-fold more fibrosis) in LV region compared with that in MR rats. These results indicated that DAPA attenuates MR-induced cardiac fibrosis in our model.

DAPA Attenuated Cardiac Apoptosis and ER Stress in MR Rats

Using TUNEL and F-actin staining, the apoptotic cardiomyocytes were identified in each group. Compared with the Sham rats, the number of apoptotic cardiomyocytes significantly increased in LV regions of MR rats (from 30% increased to 70%) and was partially suppressed by DAPA treatment (to 50%) (Figure 7A). The apoptosis-related proteins, including Bax, cleaved caspase 3, and BCL2, in cardiac tissue was measured by Western blot (Figure 7B). Compared with Sham rats, both Bax and cleaved caspase 3 were markedly upregulated in LV region

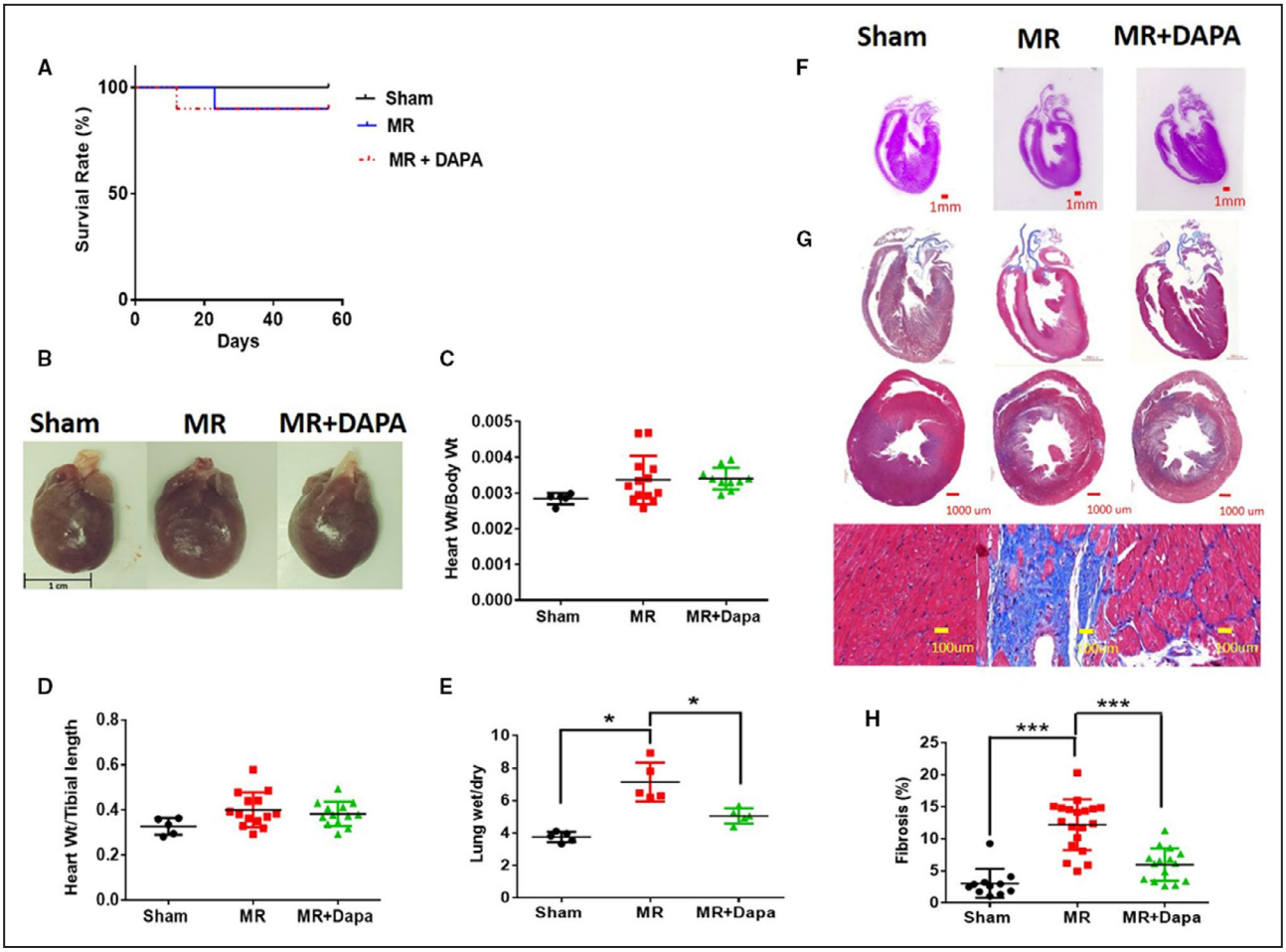

Figure 6. Dapagliflozin (DAPA) attenuated mitral regurgitation (MR)-induced cardiac injury and fibrosis.
Effects of dapagliflozin on (**A**) survival rate in the Sham, MR, and MR+DAPA groups. **B**, Representative images of harvested hearts. **C**, The quantitative analysis of heart weight/body weight, (**D**) heart weight/tibial length, (**E**) the wet to dry lung weight ratio, (**F**) hematoxylin-eosin staining of heart sections, and (**G**) Masson trichrome staining of left ventricular tissue in indicated groups; scale bars, 100 μm. **H**, Quantification of cardiac fibrosis in indicated groups of rat. Data are expressed using mean± SD. Kruskal-Wallis test and Dunn's post hoc analysis for analysis of group differences. *P<0.05, and* ***P<0.0001 for difference from each group. (N=6–12).

of MR rats, while being significantly suppressed in LV of rats treated with DAPA. Conversely, the expression of antiapoptotic protein BCL2 was significantly downregulated in LV region of MR rats but preserved in MR rats treated with DAPA.

Furthermore, we investigated whether DAPA attenuated MR-induced apoptosis through regulating ER stress pathway. The expression of ER stress-associated proteins including GRP78 (glucose-regulated protein 78), p-PERK, eIF2α, ATF4, and CHOP in cardiac tissue among each group were measure by Western blot. Compared with Sham rats, the expression of ER stress-associated proteins were significantly upregulated in MR rats, whereas those protein expressions were significantly suppressed in rats treated with DAPA (Figure 8). These results indicated that DAPA attenuates MR-induced apoptosis, an action that in part could include specific inhibition of key cardiac and ER stress and apoptosis-linked proteins.

DISCUSSION

In this study, using a mini-invasive technique we first established a novel MR model in rats to investigate thoroughly a potential protective role of DAPA in MR-induced cardiac dysfunction. We found clear cardioprotective effects of DAPA, in the setting of MR and by using a novel, rodent surgical MR model. We also established a linkage between DAPA action on MR model, and a number of key molecular pathways. The target pathways identified here, include calcium channel and gap junction proteins, along with ER stress proteins, all of which should be probed and investigated as potential mechanism of action targets

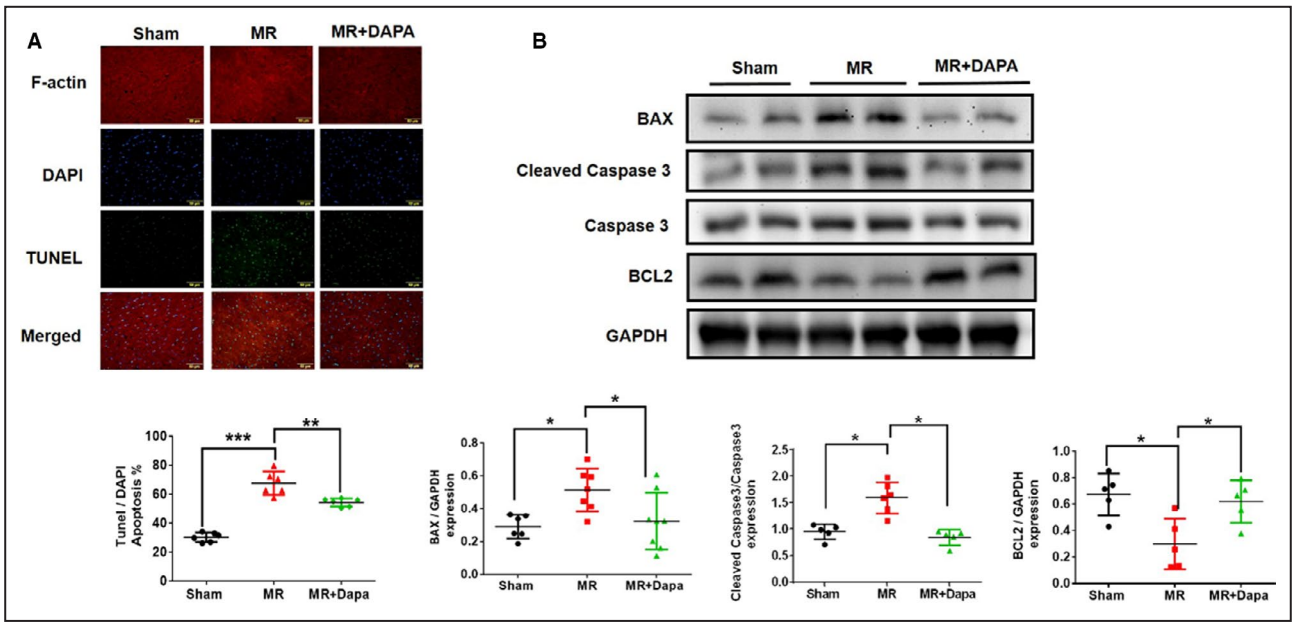

Figure 7. Dapagliflozin (DAPA) suppressed cardiomyocyte apoptosis with mitral regurgitation (MR).
A, Representative apoptotic cells by terminal deoxynucleotidyl transferase–mediated UTP nick-end labeling (TUNEL) analysis (upper panel). Quantification of cardiac apoptosis in indicated groups of rats (lower panel). (Green: TUNEL, Red: F-actin, Blue: DAPI). **B**, Expression of apoptosis associated protein were measured by Western blot. Representative BAX, cleaved caspase 3/caspase 3 ratio, and BCL2 expression in the left ventricle in each group of rats (upper panel). The relative expression level of each protein was quantified by densitometry and normalized to the GAPDH (glyceraldehyde 3-phosphate dehydrogenase) level (lower panel). Data are expressed using mean± SD. Kruskal-Wallis test and Dunn's post hoc analysis for analysis of group differences. **P*<0.05, ***P*<0.01, and ****P*<0.001 for difference from each group. (N=3–6). DAPI indicates 4', 6-diamidino-2-phenylindole; TUNEL, terminal deoxynucleotidal transferase–mediated biotin–deoxyuridine triphosphate nick-end labeling; and UTP, uridine triphosphate.

and pathways that can be differentially regulated in MR-induced HF.

Mini-Invasive MR Model in Rats

MR that induces LV volume overload is the most common type of valvular heart disease seen.[2,25] Previous research studies have tended to focus on large animal models (as in dogs and sheep).[26,27] However, such efforts are expensive and often limited by the number of animals available. Because of such constraints, some studies have established an alternative rat model of MR[28–31] but these models also have their own limitations. The open chest surgery tends to reduce the survival and success rate. In contrast to the previous established studies, here we used a novel, mini-invasive technique and created a very specific and highly localized structural defect on the leaflet of the MV, using rats. The strategy we took successfully increased the animal survival, decreased the procedure time and we hope that it provides a less invasive alternative to the more time-consuming, conventional surgical techniques like MR surgery as has been typically done in small animals.[28] Two weeks after MR creation, using echocardiography we validated our model of MR induction with imaging and indeed, as expected the technique reliably concomitant led to enlarged LA and LV chambers and resulted in systolic dysfunction, 2 weeks after the injury. We further corroborated the model by histology, which revealed overall eccentric hypertrophic cellular phenotype along with increased fibrosis. The data closely parallel what we routinely observe, clinically, in patients with MR. We believe that the rat model provides a viable and easily accessible tool for future research into MR and/or, volume overload-induced HF. Also, it can be a useful, quick, and reliable methodology for the investigation of pharmacologic therapy for MR.

Molecular Mechanisms of MR-Induced LV Remodeling

Volume overload-induced mechanical stress is detrimental to cardiomyocytes, resulting in activated inflammation and apoptosis.[3] It also induces the local production of reactive oxygen species and inflammatory cytokines.[32] In Ahmed and colleagues' work, a pathological increase of reactive oxygen species was found to be associated with myofibrillar degeneration in patients with MR.[33] Consequently, reactive oxygen species stimulates ER stress response and leads to cellular apoptosis and fibrosis.[34,35] Likewise, it has been demonstrated that ER stress-mediated

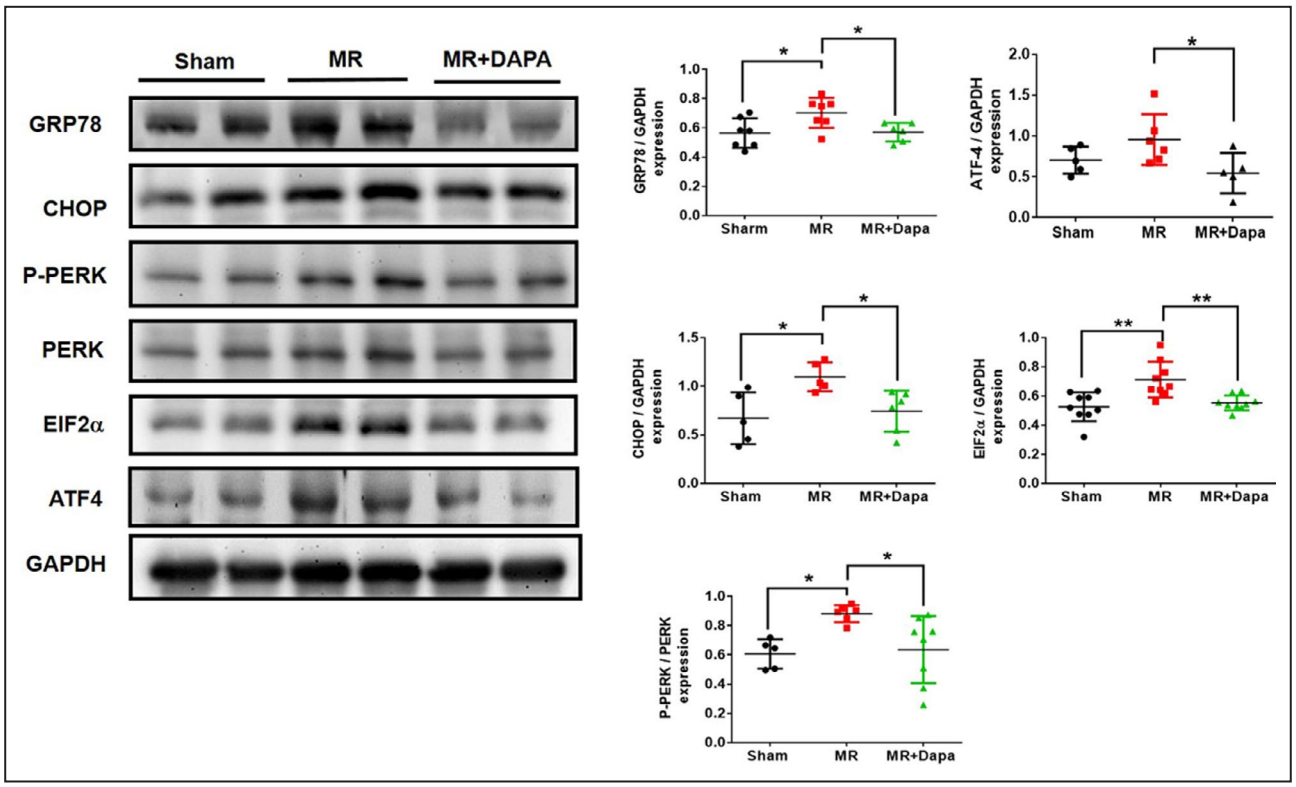

Figure 8. Dapagliflozin (DAPA) attenuates mitral regurgitation (MR) induced endoplasmic reticulum (ER) stress in hearts of rats with MR.

The expression of ER stress-associated proteins were measured by Western blot. Representative GRP78 (glucose-regulated protein 78), CHOP (C/EBP-homologous protein), p-PERK (phospho-protein kinase RNA-like endoplasmic reticulum kinase)/PERK ratio, eIF2α (eukaryotic translation initiation factor 2α), and ATF4 (activating transcription factor 6) in the left ventricles in each group of rats (left panel). The relative expression level of each protein was quantified by densitometry and normalized to the control level (right panel). Data are expressed using mean± SD. Kruskal-Wallis test and Dunn's post hoc analysis for analysis of group differences. **P*<0.05, ***P*<0.01 for difference from each group. (N=3–6).

apoptosis is an important pathway involved in AF progression.[8,36] In our rat model of MR, we observed similar increased expression of ER- and apoptosis-associated proteins, and a corresponding reduction of the aforementioned proteins, by DAPA treatment. Moreover, rats of MR exhibited a higher inducibility and maintenance of pacing-induced AF. It remains to be seen if the interplay between such molecular pathways involved in MR, and DAPA action, works to benefit the overall outcome and if ER stress-associated response is essential in development and or progression of MR.

DAPA Can be Used in the Treatment of MR in Patients

Patients with MR are often asymptomatic until severe HF ensues and this often occurs at a very late stage of the disease, resulting in longer hospitalizations, complex surgical interventions, and in many cases, a poor prognosis.[25] According to 2017 American Heart Association and European Society of Cardiology guidelines for management of MR, surgical repair or replacement of the MV is currently the only recommended therapy. Unfortunately, that treatment still cannot prevent the volume overload-induced direct cardiomyocyte injury that may have already occurred at the time of such late detection and intervention and as such, is irreversible. Although β blockers and renin-angiotensin-aldosterone system inhibitors had been prescribed in the treatment of MR, their success in relieving symptoms and delaying surgical interventions remains limited.[37] Additionally, the postoperative recurrence of AF is frequently observed in these patients and is associated with the decline in functional reserve of LA. Therefore, for all these reasons, we undertook an alternative approach, using a mini-invasive method in conjunction with a well-known therapeutic agent DAPA, to see if it is possible to mitigate the MR hemodynamic problem early, and sufficiently, and to potentially improve function and survival. Given that DAPA is used in clinic already and is an effective agent with clear glucose lowering

action, it seemed entirely plausible to see if it can also restore myocardial function in MR induction, especially if given in an early stage of disease. We conjectured that if DAPA can alleviate some of the downstream effects of MR that possibly exacerbate the pathology later, and if it can prolong a surgery-free lifestyle, it can be a useful and effective agent in the clinical HF management toolbox, to prevent adverse cardiac events and heart failure.

Through increasing glycosuria, DAPA reduces plasma glucose, blood pressure, and body weight.[38] It is currently approved by the Food and Drug Administration for the treatment of diabetes mellitus and several observations support that DAPA could be a choice for diabetic/nondiabetic cardiomyopathy, HF, and myocardial ischemia.[10,16,39] In this study, we found that DAPA treatment not only prevented progressive cardiac dysfunction but that it also attenuated cardiac fibrosis in rats with MR. It has been previously shown that DAPA works on the heart and its action on reduction in cardiac inflammation, oxidative stress, apoptosis, and mitochondrial dysfunction is also known. That said, to our knowledge, this is the first study to reveal a novel mechanism explaining its therapeutic action (Figure 9; graphic abstract). Our study corroborates previous findings, while shedding new insight into its mechanism of action. Using a new rodent surgical model and identifying new molecular connections underlying DAPA, we hope to explain the beneficial effect of DAPA through both known pathways such as inhibiting apoptosis, reducing ER stress, or newly identified pathways such as differential regulation of calcium signaling or conduction mechanics, which are induced by MR. Our findings also suggest that DAPA could be a choice agent to mitigate some of the negative impact of volume overload on LV remodeling as seen in MR and as such can help patients diagnosed with MR, especially to reduce the severity of pathology and potentially circumvent surgery by early detection and intervention and thus, MR-associated hospitalizations or death.

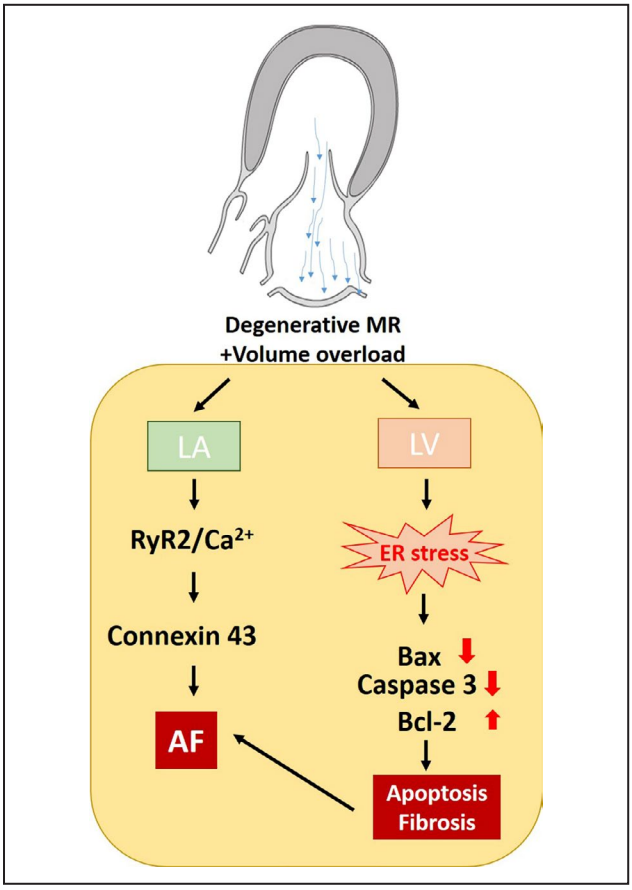

Figure 9. The summary of a postulated regulatory mechanism of action of dapagliflozin is shown to highlight its effect on improvement of mitral regurgitation (MR)-induced cardiomyopathy.
In left atrium, through differentially regulating critical proteins- by reducing RyR2 levels and increasing Connexin 43 expression, Dapagliflozin partially suppresses the inducibility of atrial fibrillation. In left ventricle, Dapagliflozin protects against MR induced apoptosis through suppressing ER stress pathway. AF indicates atrial fibrillation; ER, endoplasmic reticulum; LA, left atrium; and LV, left ventricle.

CONCLUSIONS

Collectively, our data show that DAPA improved left ventricular dysfunction, restored end-systolic pressure-volume relationship, mitigated LA inducibility and maintenance of AF. Using the same model, when we also investigated the molecular mechanism to explain its targeted action, we made a number of key observations. Molecularly, DAPA appears to exert a pleiotropic effect intersecting a number of significant molecular pathways namely (1) cardiac fibrosis, (2) cardiac ER stress, (3) ER stress-associated apoptosis, (4) electrical conduction, and (5) calcium signaling. This broad display of molecular players, which appear to correlate with DAPA action, suggests an existing molecular network that is involved in the maintenance of cardiac homeostasis. Such a potential network connection at the heart of DAPA's mechanism of action can be further probed as a cardio-protective therapy, and key targets for DAPA-specific action need to be explored in more detail. Through a combined set of approaches ranging from in vivo to ex vivo to in vitro work, this study explores the potential translational impact of DAPA use in management of MR and may be a first step toward further research study in patients with MR-induced heat failure.

ARTICLE INFORMATION

Received October 28, 2020; accepted February 8, 2021.

Affiliations

From the Division of Cardiology, Department of Internal Medicine (Y.L., J.S., Z.C., W.C.); Department of Radiology (C.C.) and Division of Cardiovascular Surgery (B.C.), Chi-Mei Medical Center, Tainan, Taiwan; Department of Biotechnology, Southern Taiwan University of Science and Technology, Tainan, Taiwan (B.C., W.C.); Department of Medical Research, Chi Mei Medical Center, Tainan, Taiwan (C.C., M.L.); Department of Hospital and Health Care Administration, Chi-Mei Medical Center, Tainan, Taiwan (C.H.); Department of Medicine, Brigham and Women's Hospital, Harvard Medical School, Boston, MA (S.F.); and Institute of Clinical Medicine, College of Medicine, National Cheng Kung University, Tainan, Taiwan (W.C.).

Acknowledgments

We especially thank the support from Professor Wei-Jan Chen in Linkou Chang Gung Memorial Hospital/Chang Gung University, Taiwan. Also, we appreciate Dr Katharina Schimmel's help in reviewing and revising this work.

Sources of Funding

This study was supported by Chi-Mei Medical Center, Ministry of Science and Technology (MOST 108-2628-B-384; 109-2326-B-384 -001 -MY3), National Health Research Institute (NHRI-EX106-10618SC).

Disclosures

None.

Supplementary Material

Figures S1–S3

REFERENCES

1. Benjamin EJ, Blaha MJ, Chiuve SE, Cushman M, Das SR, Deo R, de Ferranti SD, Floyd J, Fornage M, Gillespie C, et al.; American Heart Association Statistics Committee and Stroke Statistics Subcommittee. Heart disease and stroke statistics-2017 update: a report from the American Heart Association. *Circulation*. 2017;135:e146–e603. DOI: 10.1161/CIR.0000000000000485.
2. Adams DH, Rosenhek R, Falk V. Degenerative mitral valve regurgitation: best practice revolution. *Eur Heart J*. 2010;31:1958–1966. DOI: 10.1093/eurheartj/ehq222.
3. Anyanwu AC, Adams DH. Etiologic classification of degenerative mitral valve disease: Barlow's disease and fibroelastic deficiency. *Semin Thorac Cardiovasc Surg*. 2007;19:90–96. DOI: 10.1053/j.semtcvs.2007.04.002.
4. Wang J, Hu X, Jiang H. ER stress-induced apoptosis: a novel therapeutic target in heart failure. *Int J Cardiol*. 2014;177:564–565. DOI: 10.1016/j.ijcard.2014.08.118.
5. Hetz C, Chevet E, Harding HP. Targeting the unfolded protein response in disease. *Nat Rev Drug Discov*. 2013;12:703–719. DOI: 10.1038/nrd3976.
6. Shi J, Jiang Q, Ding X, Xu W, Wang DW, Chen M. The ER stress-mediated mitochondrial apoptotic pathway and MAPKs modulate tachypacing-induced apoptosis in HL-1 atrial myocytes. *PLoS One*. 2015;10:e0117567. DOI: 10.1371/journal.pone.0117567.
7. Müller P, Deneke T, Schiedat F, Bösche L, Strauch J, Dietrich JW, Vogt M, Tannapfel A, Stiegler H, Mügge A, et al. Increased preoperative serum apoptosis marker fas ligand correlates with histopathology and new-onset of atrial fibrillation in patients after cardiac surgery. *J Cardiovasc Electrophysiol*. 2013;24:1110–1115. DOI: 10.1111/jce.12191.
8. Chen JZ, Xie J, Li GN, He GX, Tan W, Zhu SH, Chen QH, Wu H, Zhang XL, Wang L, et al. Endoplasmic reticulum stress associated apoptosis implicated in atrial fibrillation. *Int J Clin Exp Pathol*. 2016;9:1652–1659.
9. Meyer-Roxlau S, Lämmle S, Opitz A, Künzel S, Joos JP, Neef S, Sekeres K, Sossalla S, Schöndube F, Alexiou K, et al. Differential regulation of protein phosphatase 1 (PP1) isoforms in human heart failure and atrial fibrillation. *Basic Res Cardiol*. 2017;112:43. DOI: 10.1007/s00395-017-0635-0.
10. Plosker GL. Dapagliflozin: a review of its use in patients with type 2 diabetes. *Drugs*. 2014;74:2191–2209. DOI: 10.1007/s40265-014-0324-3.
11. Jung CH, Jang JE, Park JY. A novel therapeutic agent for type 2 diabetes mellitus: SGLT2 inhibitor. *Diabetes Metab J*. 2014;38:261–273. DOI: 10.4093/dmj.2014.38.4.261.
12. Nakagawa Y, Kuwahara K. Sodium-glucose cotransporter-2 inhibitors are potential therapeutic agents for treatment of non-diabetic heart failure patients. *J Cardiol*. 2020;76:123–131. DOI: 10.1016/j.jjcc.2020.03.009.
13. McMurray JJV, DeMets DL, Inzucchi SE, Køber L, Kosiborod MN, Langkilde AM, Martinez FA, Bengtsson O, Ponikowski P, Sabatine MS, et al. A trial to evaluate the effect of the sodium-glucose co-transporter 2 inhibitor dapagliflozin on morbidity and mortality in patients with heart failure and reduced left ventricular ejection fraction (DAPA-HF). *Eur J Heart Fail*. 2019;21:665–675. DOI: 10.1002/ejhf.1432.
14. Kim YG, Han SJ, Kim DJ, Lee KW, Kim HJ. Association between sodium glucose co-transporter 2 inhibitors and a reduced risk of heart failure in patients with type 2 diabetes mellitus: a real-world nationwide population-based cohort study. *Cardiovasc Diabetol*. 2018;17:91. DOI: 10.1186/s12933-018-0737-5.
15. Lunder M, Janic M, Japelj M, Juretic A, Janez A, Sabovic M. Empagliflozin on top of metformin treatment improves arterial function in patients with type 1 diabetes mellitus. *Cardiovasc Diabetol*. 2018;17:153. DOI: 10.1186/s12933-018-0797-6.
16. Wiviott SD, Raz I, Bonaca MP, Mosenzon O, Kato ET, Cahn A, Silverman MG, Zelniker TA, Kuder JF, Murphy SA, et al. Dapagliflozin and cardiovascular outcomes in type 2 diabetes. *N Engl J Med*. 2019;380:347–357. DOI: 10.1056/NEJMoa1812389.
17. Tanajak P, Sa-Nguanmoo P, Sivasinprasasn S, Thummasorn S, Siri-Angkul N, Chattipakorn SC, Chattipakorn N. Cardioprotection of dapagliflozin and vildagliptin in rats with cardiac ischemia-reperfusion injury. *J Endocrinol*. 2018;236:69–84. DOI: 10.1530/JOE-17-0457.
18. Yurista SR, Sillje HHW, Oberdorf-Maass SU, Schouten EM, Pavez Giani MG, Hillebrands JL, van Goor H, van Veldhuisen DJ, de Boer RA, Westenbrink BD. Sodium-glucose co-transporter 2 inhibition with empagliflozin improves cardiac function in non-diabetic rats with left ventricular dysfunction after myocardial infarction. *Eur J Heart Fail*. 2019;21:862–873. DOI: 10.1002/ejhf.1473.
19. Byrne NJ, Parajuli N, Levasseur JL, Boisvenue J, Beker DL, Masson G, Fedak PWM, Verma S, Dyck JRB. Empagliflozin prevents worsening of cardiac function in an experimental model of pressure overload-induced heart failure. *JACC Basic Transl Sci*. 2017;2:347–354. DOI: 10.1016/j.jacbts.2017.07.003.
20. Zhou Y, Wu W. The sodium-glucose co-transporter 2 inhibitor, empagliflozin, protects against diabetic cardiomyopathy by inhibition of the endoplasmic reticulum stress pathway. *Cell Physiol Biochem*. 2017;41:2503–2512. DOI: 10.1159/000475942.
21. Shibusawa R, Yamada E, Okada S, Nakajima Y, Bastie CC, Maeshima A, Kaira K, Yamada M. Dapagliflozin rescues endoplasmic reticulum stress-mediated cell death. *Sci Rep*. 2019;9:9887. DOI: 10.1038/s41598-019-46402-6.
22. Lissoni A, Hulpiau P, Martins-Marques T, Wang N, Bultynck G, Schulz R, Witschas K, Girao H, De Smet M, Leybaert L. RyR2 regulates Cx43 hemichannel intracellular Ca^{2+}-dependent activation in cardiomyocytes. *Cardiovasc Res*. 2021;117:123–136. DOI: 10.1093/cvr/cvz340.
23. Basheer WA, Shaw RM. Connexin 43 and CaV1.2 ion channel trafficking in healthy and diseased myocardium. *Circ Arrhythm Electrophysiol*. 2016;9:e001357. DOI: 10.1161/CIRCEP.115.001357.
24. Borger MA, Mansour MC, Levine RA. Atrial fibrillation and mitral valve prolapse: time to intervene? *J Am Coll Cardiol*. 2019;73:275–277. DOI: 10.1016/j.jacc.2018.11.018.
25. Darby AE, Dimarco JP. Management of atrial fibrillation in patients with structural heart disease. *Circulation*. 2012;125:945–957. DOI: 10.1161/CIRCULATIONAHA.111.019935.
26. Zheng J, Chen Y, Pat B, Dell'Italia LA, Tillson M, Dillon AR, Powell PC, Shi KE, Shah N, Denney T, et al. Microarray identifies extensive downregulation of noncollagen extracellular matrix and profibrotic growth factor genes in chronic isolated mitral regurgitation in the dog. *Circulation*. 2009;119:2086–2095. DOI: 10.1161/CIRCULATIONAHA.108.826230.
27. Mishra YK, Mittal S, Jaguri P, Trehan N. Coapsys mitral annuloplasty for chronic functional ischemic mitral regurgitation: 1-year results. *Ann Thorac Surg*. 2006;81:42–46. DOI: 10.1016/j.athoracsur.2005.06.023.
28. Kim KH, Kim YJ, Ohn JH, Yang J, Lee SE, Lee SW, Kim HK, Seo JW, Sohn DW. Long-term effects of sildenafil in a rat model of chronic mitral regurgitation: benefits of ventricular remodeling and exercise capacity. *Circulation*. 2012;125:1390–1401. DOI: 10.1161/CIRCULATIONAHA.111.065300.
29. Pu M, Gao Z, Li J, Sinoway L, Davidson WR Jr. Development of a new animal model of chronic mitral regurgitation in rats under transesophageal

echocardiographic guidance. *J Am Soc Echocardiogr*. 2005;18:468–474. DOI: 10.1016/j.echo.2004.10.005.
30. Kim KH, Kim YJ, Lee SP, Kim HK, Seo JW, Sohn DW, Oh BH, Park YB. Survival, exercise capacity, and left ventricular remodeling in a rat model of chronic mitral regurgitation: serial echocardiography and pressure-volume analysis. *Korean Circ J*. 2011;41:603–611. DOI: 10.4070/kcj.2011.41.10.603.
31. Pu M, Gao Z, Zhang X, Liao D, Pu DK, Brennan T, Davidson WR Jr. Impact of mitral regurgitation on left ventricular anatomic and molecular remodeling and systolic function: implication for outcome. *Am J Physiol Heart Circ Physiol*. 2009;296:H1727–H1732. DOI: 10.1152/ajpheart.00882.2008.
32. Gealekman O, Abassi Z, Rubinstein I, Winaver J, Binah O. Role of myocardial inducible nitric oxide synthase in contractile dysfunction and beta-adrenergic hyporesponsiveness in rats with experimental volume-overload heart failure. *Circulation*. 2002;105:236–243. DOI: 10.1161/hc0202.102015.
33. Ahmed MI, Gladden JD, Litovsky SH, Lloyd SG, Gupta H, Inusah S, Denney T Jr, Powell P, McGiffin DC, Dell'Italia LJ. Increased oxidative stress and cardiomyocyte myofibrillar degeneration in patients with chronic isolated mitral regurgitation and ejection fraction >60%. *J Am Coll Cardiol*. 2010;55:671–679. DOI: 10.1016/j.jacc.2009.08.074.
34. Schroder M, Kaufman RJ. The mammalian unfolded protein response. *Annu Rev Biochem*. 2005;74:739–789. DOI: 10.1146/annurev.biochem.73.011303.074134.
35. Minamino T, Komuro I, Kitakaze M. Endoplasmic reticulum stress as a therapeutic target in cardiovascular disease. *Circ Res*. 2010;107:1071–1082. DOI: 10.1161/CIRCRESAHA.110.227819.
36. Wiersma M, Meijering RAM, Qi XY, Zhang D, Liu T, Hoogstra-Berends F, Sibon OCM, Henning RH, Nattel S, Brundel B. Endoplasmic reticulum stress is associated with autophagy and cardiomyocyte remodeling in experimental and human atrial fibrillation. *J Am Heart Assoc*. 2017;6:e006458. DOI: 10.1161/JAHA.117.006458.
37. Slipczuk L, Rafique AM, Davila CD, Beigel R, Pressman GS, Siegel RJ. The role of medical therapy in moderate to severe degenerative mitral regurgitation. *Rev Cardiovasc Med*. 2016;17:28–39.
38. Thomas MC, Cherney DZI. The actions of SGLT2 inhibitors on metabolism, renal function and blood pressure. *Diabetologia*. 2018;61:2098–2107. DOI: 10.1007/s00125-018-4669-0.
39. Furtado RHM, Bonaca MP, Raz I, Zelniker TA, Mosenzon O, Cahn A, Kuder J, Murphy SA, Bhatt DL, Leiter LA, et al. Dapagliflozin and cardiovascular outcomes in patients with type 2 diabetes mellitus and previous myocardial infarction. *Circulation*. 2019;139:2516–2527. DOI: 10.1161/CIRCULATIONAHA.119.039996.

SUPPLEMENTAL MATERIAL

Figure S1. Effects of Dapagliflozin (DAPA) on (A) body weight, (B) blood glucose, (C) heart rate and (D-F) blood pressures in the Sham, MR, and MR+ DAPA groups.

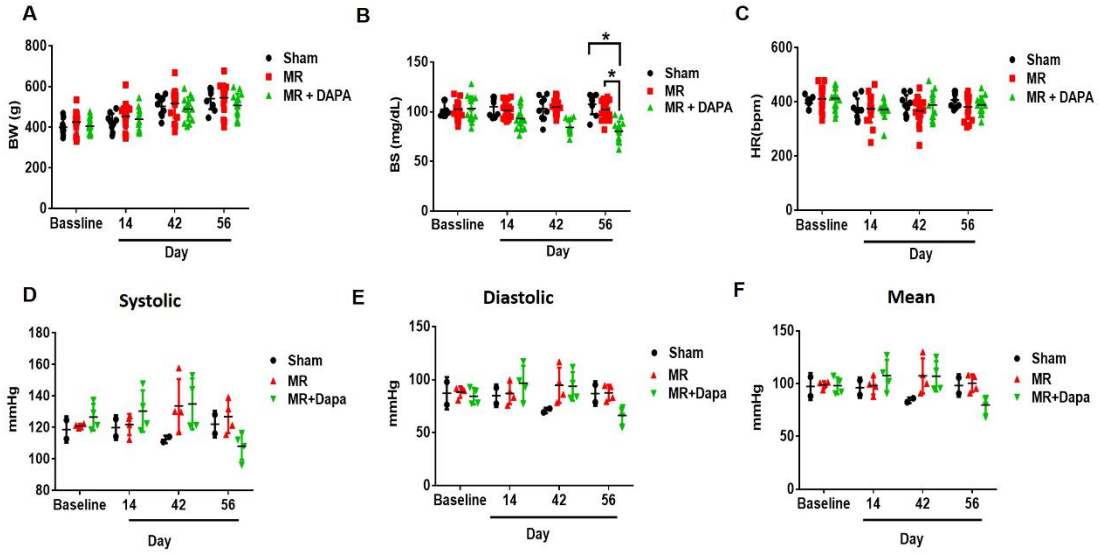

Data are expressed using mean ± standard deviation (S.D.). Kruskal-Wallis test and Dunn's post-hoc analysis for analysis of group differences. *$P < 0.05$ for difference from each group. (N=6-12).

Figure S2. Echocardiographic assessment of Dapagliflozin (DAPA) treatment on mitral regurgitation (MR) induced diastolic dysfunction.

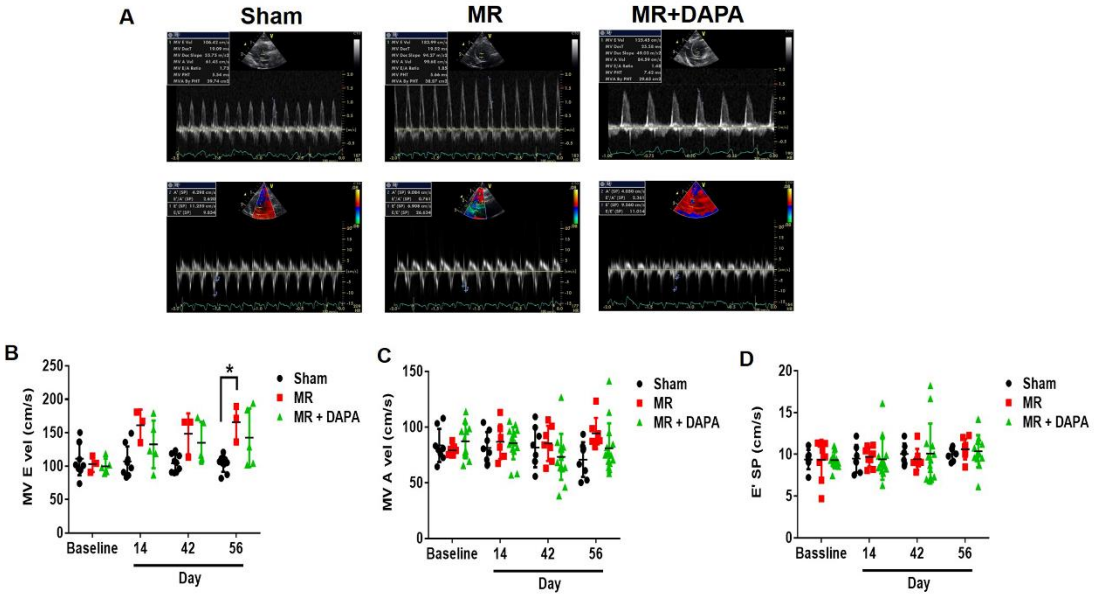

(**A**) Sequential measurements of echocardiography are shown in the Sham, MR and MR+ DAPA groups. Echocardiographic measurements of (**B**) transmitral early filling velocity, (**C**) atrial velocity and (**D**) tissue Doppler derived early (e′) annular diastolic velocities are shown for each group. Data are expressed using mean ± standard deviation (S.D.). Kruskal-Wallis test and Dunn's post-hoc analysis for analysis of group differences. *$P < 0.05$ for difference from each group. (N=6-9)

Figure S3. Electrocardiographic assessment of at baseline and the end of experiments of rats of the Sham, mitral regurgitation (MR) and MR+ Dapagliflozin (DAPA).

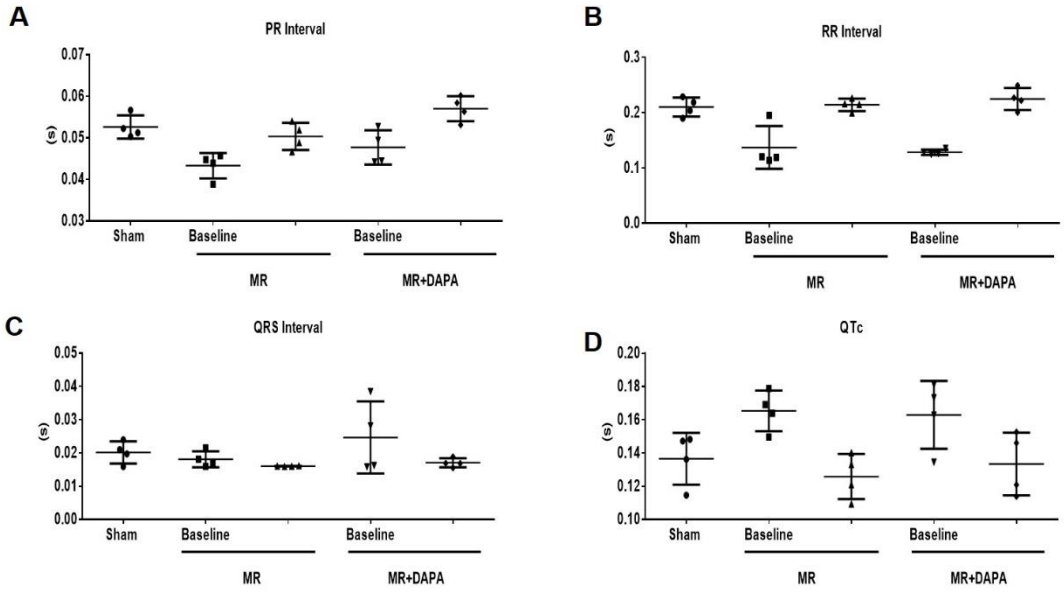

(**A**) PR intervals, (**B**) RR intervals, (**C**) QRS durations and (**D**) QTc intervals. (N=3-6).